KSCE Journal of Civil Engineering (0000) 00(0):1-10
DOI 10.1007/s12205-015-0235-1

Geotechnical Engineering
pISSN 1226-7988, eISSN 1976-3808
www.springer.com/12205

Numerical Modeling of the Seismic Racking Behavior of Box Culverts in Dry Cohesionless Soils

Ozgur L. Ertugrul*

Received May 9, 2014/Revised October 29, 2014/Accepted July 29, 2015/Published Online August 31, 2015

Abstract

In this study, dynamic behavior and lateral earth pressures on box shaped culverts buried in dry cohesionless soils were investigated through validated numerical analyses. Two dimensional plane strain finite difference models of 4m-high box culverts with different wall flexibilities were analyzed using FLAC-2D Finite Difference Code. The effect of relative flexibility on the dynamic racking displacements of the structure was investigated by modifying dynamic shear modulus of the cohesionless soil and structural attributes of the models. Shear strains, horizontal accelerations and wall deformations as well as lateral dynamic earth pressures at various points on the culvert were investigated through the numerical analyses. Results of the numerical analyses were validated with those of a previous centrifuge modeling study. Racking deformations of the numerical culvert models are found to be in agreement with the centrifuge test data. Dynamic lateral pressures acting on the side walls increase as the wall flexibility ratio decreases. Dynamic force on the sidewalls of the box culvert may reach up to 2.8 times the at-rest lateral earth load for the stiff prototype, whereas for the flexible prototype, this value is only 1.6 times the static earth load.

Keywords: *Box culvert, numerical model, racking, lateral pressure, relative flexibility, cohesionless soil*

1. Introduction

Box structures buried in soils may experience transverse racking deformations due to the shear distortions of the ground during earthquakes. Dynamic shear deformations of the soils affect box culverts in the form of dynamic shear stresses and normal pressures induced along the culvert walls, roof and bottom slabs. Wall stiffness and interface friction play an important role on the induced stresses. These dynamic forces and stresses are superimposed on the existing static state of stress in the structural members by disturbing the structural integrity of the box culverts. Damages to shallow buried cut-and-cover structures, including regular box sections were reported during the earthquakes of 1906 San Francisco and 1971 San Fernando (Owen and Scholl, 1981). The damages included longitudinal cracks along the walls, failure at the top and bottom wall joints and failure of longitudinal construction joints.

During the last decades, seismic behavior of circular culverts was investigated using centrifuge tests and numerical analyses. Based on these studies, empirical and semi-empirical methods were suggested to estimate the soil pressures, structural stresses and deflections of circular sections. On the other hand, there is very little research on the seismic response of box culverts with shallow to moderate depth installations. Currently, deformation based methods play a major role in the earthquake resistant design of buried structures since these approaches are more successful in estimating the seismic racking deformations of the box-shaped buried structures in a more realistic way compared to methods based on rigid block analysis. Various versions of this approach are now included in the seismic design codes of countries including Korea, Japan and United States. Free-field deformation approach is one of the most common within deformation based methodologies. This approach is based on the assumption that the structure moves in accordance with the soil during seismic excitation. In other words, strains of the surrounding ground under seismic waves are directly applied to the rectangular underground structure. Although this method provides good approximations of the structural response, soil-structure interaction effect is not taken into account. Inertial effects significantly affect displacements in the surrounding soil in case of rigid underground structures. Therefore, seismic deformations may be underestimated or overestimated depending on the relative stiffness of the structure (Wang, 1993). In order to take into account soil structure interaction effect, Wang (1993), Penzien (2000) and Huo *et al.* (2006) suggested different versions of Simplified Frame Analysis (SFA) method. In SFA approach, unit racking deformations of the structure are estimated by considering the relative stiffness of the structure and those deformations are applied as a static load to compute sectional forces. Structural analysis techniques were used to determine

*Assistant Professor, Dept. of Civil Engineering, Mersin University, P.O. Box 33343, Mersin, Turkey (Corresponding Author, E-mail: ozgurertugrul@hotmail.com)

sectional forces.

Physical model tests performed on reduced scale box culvert models play an important role for investigating the actual dynamic response of these structures and improving the current analytical approaches available in the seismic design codes. In a recent study, Ulgen (2011) performed dynamic centrifuge tests on buried rectangular culverts in IFFSTAR Centrifuge Facility in France which is a member of Seismic Engineering Research Infrastructures for European Synergies. Dynamic racking behavior of the box-type underground culverts and the effect of culvert relative stiffness on the dynamic pressures were investigated. Seismic pressure coefficients were suggested for different relative flexibility ratios. In a more recent study, Debiasi *et al.* (2013) performed parametric finite element analyses to investigate the interface friction effects and aspect ratio on the seismic response of shallow buried rectangular frames and culverts. They found that non-linear interface friction significantly affects the seismic behavior of shallow buried structures however, as the burial depth increases, interface effects cease. The effect of aspect ratio of the structure also diminishes beyond a critical depth and the soil-structure interface may be assumed as perfectly tied. In their numerical analyses, soil stiffness and damping were assumed as constant within the soil profile. Although, Wang (1993) and Bobet *et al.* (2008) assume constant dynamic properties within the soil profile for their analyses, it is highly unlikely that there will not be any softening and stiffness reduction in the soil due to increasing soil strains during earthquakes.

2. Aim of the Study

The present study discusses results of a series of numerical analyses addressing the dynamic behavior of box shaped culverts embedded in cohesionless soils. Two dimensional finite difference models of a full scale box culvert were analyzed considering plane strain condition. Time dependent racking deformations of the culverts and dynamic lateral earth pressures on the side walls of the structure were monitored in the numerical analyses. Numerical model used in this study was validated against the results of a previous dynamic centrifuge tests presented by Ulgen (2011) and Ozkan *et al*. (2013).

3. Methodology of the Study

Numerical analyses were performed with two dimensional explicit FLAC v6.0 (Itasca, 2008) finite difference code. Prototype dimensions of the culvert models used in the centrifuge tests performed by Ulgen (2011) were adopted in the numerical analyses. The dynamic lateral culvert deformations and shear strains monitored during centrifuge tests served for the calibration and validation of the finite difference model. Mechanical properties of the backfill material and structural attributes of the culvert models used in the numerical modeling were taken in accordance with the values reported by Ozkan *et al.* (2013). Different from the previous work reported in the literature, in the current study, stiffness degradation and damping ratio of the soil were adopted as a function of soil strains and confining stress to represent the actual behavior in a more realistic way.

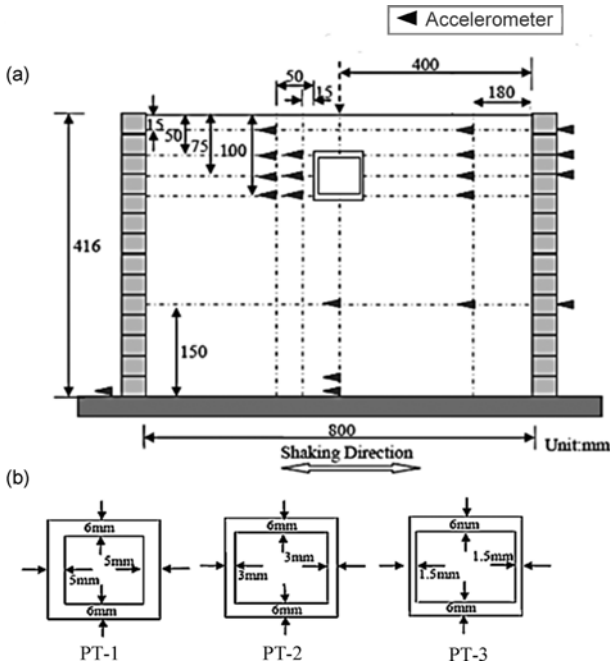

Fig. 1. (a) Centrifuge Test Set-up and (b) Cross-sectional View of the Culvert Models (Ozkan *et al.*, 2013)

3.1 Overview of the Centrifuge Test Set-up

The centrifuge test set-up and the locations of the acceleration transducers in the backfill were shown in Fig. 1(a). Culvert models having different Initial Flexibility Ratio (IFR) were tested in the centrifuge facility. According to Wang (1993), *IFR* was defined as the relative stiffness of the underground structure with respect to the non-deformed soil and given by:

$$IFR = \frac{G_{max} W}{SH} \tag{1}$$

where G_{max} is the maximum shear modulus of the soil, W and H are the width and height of the box culvert and S is the force required for unit racking deformation of the structure itself. For single barrel tubes, Eq. (1) can be expressed as:

$$IFR = \frac{G_{max}}{24}\left(\frac{H^2 W}{EI_W} + \frac{HW^2}{EI_R}\right) \tag{2}$$

where I_W and I_R are the moment of inertia of the sidewalls and top-bottom slabs. As depicted in Fig. 1(b), thickness of the roof and base slabs were relatively thick and stiff in order to eliminate structural effects due to bending. In Table 1, model and prototype dimensions of the centrifuge models were given. Standard dimensions for precast concrete box culverts used in the field applications are available in widths varying from 180 cm to 480 cm and heights between 120 cm and 420 cm. Elastic modulus of the concrete for an average compressive strength of

Table 1. Model and Prototype Dimensions for 40-g Centrifuge Environment (Ozkan *et al.*, 2013)

Model Dimension (mm)				Prototype Dimension (m)			
External		Internal		External		Internal	
Vertical	Horizontal	Vertical	Horizontal	Vertical	Horizontal	Vertical	Horizontal
50	47	38	44	2.00	1.88	1.52	1.76
50	50	38	44	2.00	2.00	1.52	1.76
50	54	38	44	2.00	2.16	1.52	1.76

Table 2. Dynamic Excitation Characteristics in Model and Prototype Scale (Ozkan *et al.*, 2013)

Excitation No. (E)	Model			Prototype		
	a_{max} (g)	f (Hz)	Duration (s)	a_{max} (g)	f (Hz)	Duration (s)
1	10	80	0.88	0.25	2	35.2
2	16	80	0.88	0.4	2	35.2
3	10	140	0.5	0.25	3.5	20
4	16	140	0.5	0.4	3.5	20

35 MPa is determined as 23.25 GPa with the following equation:

$$E_c = 57000\sqrt{f_c} \tag{3}$$

where f_c is the compressive strength of concrete in psi. Considering the typical dimensions of the culverts used in practice, most flexible section has dimensions of $H \times W$ = 420 cm × 480 cm, t_w = 20 cm and t_r = 30 cm where t_w and t_r are the plane strain thicknesses of the culvert walls and roof-bottom slabs respectively. Initial Flexibility (IFR) ratio for the most flexible section is determined as 16.97 by using Eq. (2). The most rigid section among the standard box culvert sections has dimensions of $H \times W$ = 120 cm × 180 cm, t_w = 28 cm and t_r = 30 cm. *IFR* for the most rigid concrete section is determined as 0.314. Within the scope of the study, model culverts having *IFR* values between 0.54 and 14.06 were tested (Ozkan *et al.*, 2013). This *IFR* range is representative for approximately 80% of the flexibility ratio for the actual concrete box culverts used in the field practice. In the current study, the prototype-1 (*PT-1*) with *IFR* = 0.54 is considered as the rigid model, *PT-2* having *IFR* = 2.07 as the intermediate model and *PT-3* with *IFR* = 14.06 as the flexible model.

In the dynamic tests, culvert models were subjected to harmonic base motions (Ozkan *et al*., 2013). Excitation characteristics (acceleration amplitude, predominant frequency and duration) for small scale centrifuge model (1/40 scale) and corresponding values at the prototype scale were presented in Table 2. The shaking table used for the tests has the ability to apply random motions or previous earthquake records to the test models however; harmonic base excitations were applied to be able to make valid quantitative comparisons between different culvert models (Ozkan *et al*., 2013). According to scaling relationships proposed by Iai (1989), 80 Hz frequency at 40-g centrifugal acceleration corresponds to 2 Hz at prototype scale. Based on the scaling relationships, frequency range of the tests at prototype scale is between 2 Hz and 3.5 Hz. According to Bathurst *et al.* (1998), frequencies between 2 Hz and 3 Hz are representative for typical predominant frequencies for medium to high frequency earthquakes and falls within the expected earthquake parameters for seismic design of structures in North America (AASTHO, 2002). The acceleration amplitudes of the dynamic excitations applied to the models at prototype scale (0.25 g to 0.40 g) are representative for strong earthquakes according to Wald *et al.* (1996) and Japan Meteorological Agency Seismic Intensity Scale.

The model backfill was prepared with dry pluviation technique to achieve relative density of approximately 70%. Ozkan *et al.* (2013) indicated that dry Fontainebleau sand was used in the centrifuge tests. The maximum and minimum unit weight of the material was reported as 13.93 kN/m^3 and 16.78 kN/m^3 with a specific gravity of 2.64. Peak internal friction angle of the cohesionless soil was determined as 38° based on consolidated undrained triaxial compression test results. In the triaxial tests, cylindrical specimens were prepared at the same relative density to be consistent with the initial relative density of the material in the centrifuge tests. During the dynamic phase of the centrifuge modeling, in-flight Cone Penetration Tests (CPT) were performed to monitor the changes in the relative density. Ozkan *et al.* (2013) indicated that any significant change in the relative density was not observed in the dynamic tests hence internal friction angle of 38° at 70% relative density is considered as representative for all of the physical tests. The triaxial compression tests were performed for 28 kPa all-around pressure that represents the effective confining pressure at mid-depth of prototype culvert model. The dilatancy angle of the granular materials with internal friction angle greater than 30° can be estimated by the relationship $\psi = \phi$-30° (Bozorgzadeh *et al*., 2007 and Plaxis, 1998). Hence, in the numerical analyses, internal friction angle (ϕ) and dilatation angle (ψ) are taken as 38° and 8°, respectively.

Shear modulus degradation and damping ratio curves were formulized with the following set of equations based on the empirical relationships proposed by Ishibashi and Zhang (1993):

$$\frac{G}{G_{max}} = K(\gamma)\sigma_c^{m(\gamma)-m_o} \tag{4}$$

$$K(\gamma) = 0.5\left[1 + tanh\left\{ln\left(\frac{0.000102}{\gamma}\right)^{0.613}\right\}\right] \tag{5}$$

$$m(\gamma) = m_0 = 0.34\left[1 - tanh\left\{ln\left(\frac{0.000556}{\gamma}\right)^{0.4}\right\}\right] \quad (6)$$

$$D = 25.3\left[0.513\left(\frac{G}{G_{max}}\right)^2 - 1.351\left(\frac{G}{G_{max}}\right) + 1\right] \quad (7)$$

where γ is the shear strain, K(γ) and m(γ) are functions depending on γ. m_0 is the value of the function at small strain (i.e. $m_0 = m(\gamma \leq 10^{-6})$). The maximum shear modulus (G_{max}) of Fontainebleau sand was estimated by using the following empirical relationship [Eq. (8)] proposed by Hardin and Drnevich (1970):

$$G_{max} = 3230\left(\frac{2,973 - e}{1 + e}\right)^2 OCR^k \sqrt{(\sigma'_m)} \quad (8)$$

where e is the void ratio, OCR is the over-consolidation ratio, k is an over-consolidation ratio exponent and σ'_m is the effective confining pressure in kPa. For average void ratio of 0.64 (R_d = 70%) and confining pressure of 28 kPa, the effective confining pressure at mid-depth of culvert model, G_{max} at mid-depth of culvert model was approximately calculated as approximately 56500 kPa.

3.2 Finite Difference Model

Numerical analyses were performed by adopting the prototype dimensions indicated in Table 1. The soil was modeled as homogeneous isotropic elasto-plastic material characterized by Mohr-Coulomb yield function with non-associated plastic flow rule. The internal angle of friction (ϕ) and dilatancy angle (ψ) were assigned based on test results reported by Ozkan *et al.* (2013). For all of the geomaterial sets, a nominal cohesion value (0.01 kPa) was adopted to increase the stability of the numerical solution.

In the finite difference model, the culvert structure was represented by elastic beam-column elements whereas the soil medium was modeled with quadrilateral elements. Within the analyses, elastic modulus and unit weight of the culvert material is taken as 7.1×10^7 kPa and 26.8 kN/m^3. Localized grid refinement was applied in the vicinity of the underground structure to increase the accuracy of the monitored parameters within this zone. Numerical analyses were performed with incremental loading procedure to facilitate proper simulation of geostatic stress conditions in the soil, installation process of the culvert and stress redistribution after installation of the box culvert structure. The finite difference grid and initial boundary conditions are shown in Fig. 2. Numerical analyses were performed for three different culvert wall thicknesses to investigate the effect of relative flexibility on the wall deformations and lateral pressures on the structure. Mechanical attributes of the structural elements were presented in Table 3.

Debiasi *et al.* (2013) indicates that effect of wall friction gains importance after a critical depth D_{co}, measured from ground surface to the top slab of the embedded structure. D_{co} is found to vary between 0.8L and 1.0L where L is the length of the side wall

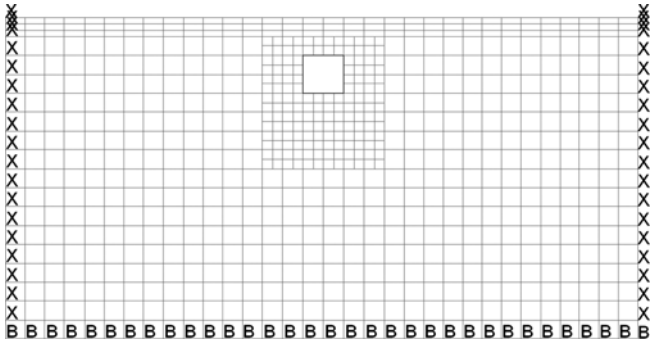

Fig. 2. Finite Difference Grid used in the Numerical Modeling

Table 3. Structural Attributes of Prototype (PT) Culverts

	Property	Sidewall	Top-Bottom slabs
PT-1	Thickness (t_w) [mm]	60	240
	Moment of Inertia (I) [m^4]	1.80×10^{-5}	1.15×10^{-3}
	k_l (kN/m)	1960	
	IFR	14.06	
PT-2	Thickness (t_w) [mm]	120	240
	Moment of Inertia (I) [m^4]	1.441×10^{-4}	1.15×10^{-3}
	k_l (kN/m)	13086	
	IFR	2.07	
PT-3	Thickness (t_w) [mm]	200	320
	Moment of Inertia (I) [m^4]	1.441×10^{-4}	1.15×10^{-3}
	k_l (kN/m)	37963	
	IFR	0.54	

for box culverts having aspect ratio of 1. Considering the low overburden depth of the models in the current study, wall-soil interfaces were not taken as fixed. Hence, elasto-plastic Mohr-Coulomb interface elements were introduced at the wall-soil contacts. Tiwari *et al.* (2010) conducted physical laboratory tests to investigate strength reduction at the interfaces between various soils and construction materials such as concrete, steel and wood. δ/ϕ ratio for sand-steel interfaces is suggested as 0.79 where δ is the interface friction angle and ϕ is the internal angle of friction for the granular material. In the numerical analyses, δ is taken as 30° for the soil-box culvert interfaces considering the δ/ϕ ratio (between sand and steel) suggested by Tiwari *et al.* (2010). Although culvert models are made of aluminum, interface reduction factor for steel is adopted in the numerical analyses since aluminum and steel has similar roughness coefficients.

Tiwari *et al.* (2010) suggests δ/φ ratio for the sand-concrete interfaces as 0.94 which is approximately 20% higher than the value taken for sand-steel interfaces. Hence, strength reduction at the soil-structure contacts for the actual box culvert sections used in field practice will be lower compared to those of the numerical analyses. Debiasi *et al.* (2013) indicated that racking ratio of the square box culverts decreases as the interface between soil and structure becomes more rigid. This effect becomes more pronounced as the burial depth of the structure decreases. Considering that the focus of the current study is on shallow buried culverts, the

racking ratio values presented in this paper stay on the conservative side since expected frictional forces induced on the actual culverts made of concrete will be higher compared to those acting on the culvert models utilized in the tests. This translates into a positive effect on reducing the earthquake induced racking deformation of the actual box culverts made of concrete.

In the dynamic analysis phase, the entire soil-structure system was subjected to harmonic horizontal velocity time histories applied to lower most grid points, to simulate earthquake-induced vertically propagating shear waves. As a result, lateral shear displacements occur within the soil. At the beginning of the dynamic phase, velocity waves were increased in small increments up to the maximum amplitude in order to reduce the effect of impact loading on the behavior of the physical models. Similarly, velocity amplitude is reduced in small increments at the end of the dynamic phase. Silent boundary conditions were applied to the limits of the model to simulate wave propagation to outside of the model geometry. The velocity waves applied at the base of the model in the x-direction have amplitudes of 0.111 m/s and 0.178 m/s. Although the application of random earthquake excitations in physical modeling studies is considered more realistic, Bathurst and Hatami (1998) and Matsuo *et al.* (1998) reported that simple harmonic base excitations cause more aggressive impact on the structure compared to the effect of a real earthquake excitation with similar predominant frequency and amplitude. Additionally, application of harmonic base motion allows more accurate comparisons to be made regarding the effect of different input excitation parameters investigated in this study.

Damping is introduced to the numerical model in hysteretic form. Shear modulus degradation and damping ratio functions given in Eqs. (4) to (7) were converted into sigmoidal functions by implementing a FISH language code to FLAC 2-D to estimate the modulus degradation and damping data within the analyses.

4. Discussion of the Results

In Fig. 3, lateral cyclic deformations of the prototype culvert PT-1 were compared with those generated by numerical analyses. A portion of deformation time histories recorded by horizontal extensometers (named as HE6 to HE9 starting from the lowermost to the uppermost extensometer, respectively according to Ozkan *et al.*, 2013) were depicted in Fig. 3(a). Extensometers were installed at equal intervals along the side walls at the middle of the overall box culvert length. Numerical model successfully replicated the actual displacements of the culvert. Peak positive and negative deformations of the culvert model as depicted in vector form in Fig. 4 were marked in ovals on the time history plotted in Fig. 3(b).

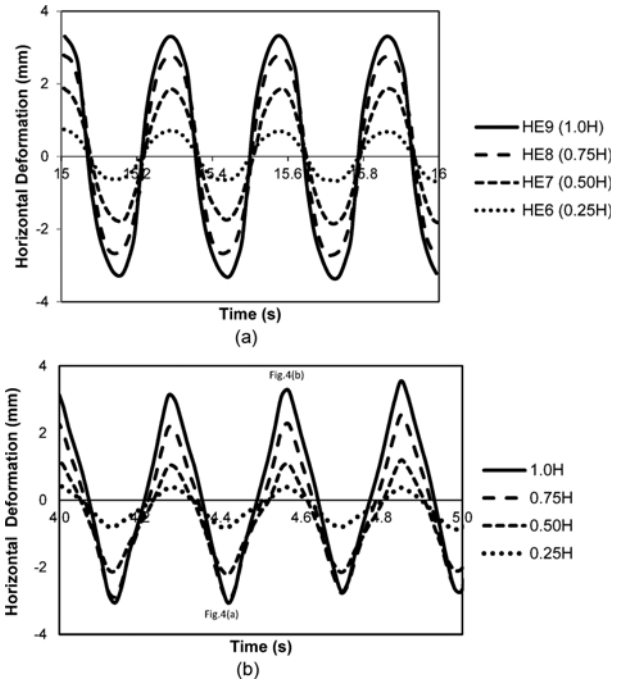

Fig. 3. Cyclic Racking Deformations of PT-1: (a) Centrifuge Test (E2), (b) Numerical Analysis

According to Ozkan *et al.* (2013), displacements of the centrifuge models were calculated in an indirect way, through integrating twice the acceleration time histories. Average shear strain between the two successive accelerometers was calculated by using first order approximation as shown in Eq. (9):

$$\gamma = \frac{\delta_2 - \delta_1}{h_2 - h_1} \tag{9}$$

where γ is the shear strain, δ_1, δ_2 are the displacements at points 1, 2 and h_1, h_2 are the depths of points 1, 2, respectively. If there

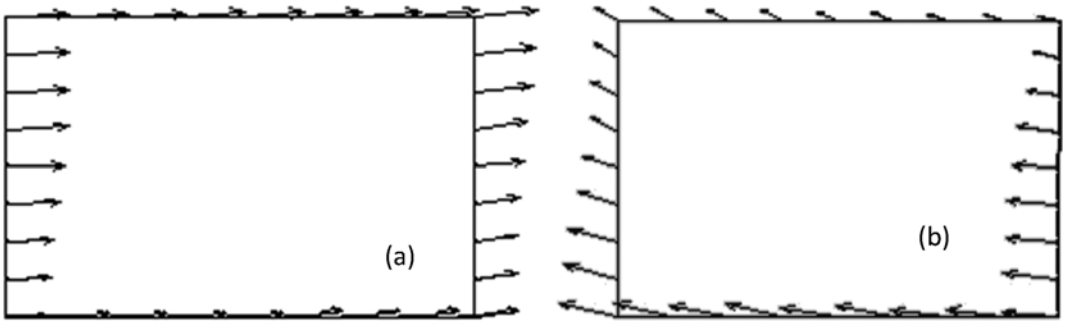

Fig. 4. Culvert Displacement Vectors at: (a) t = 4.42s, (b) t = 4.56s

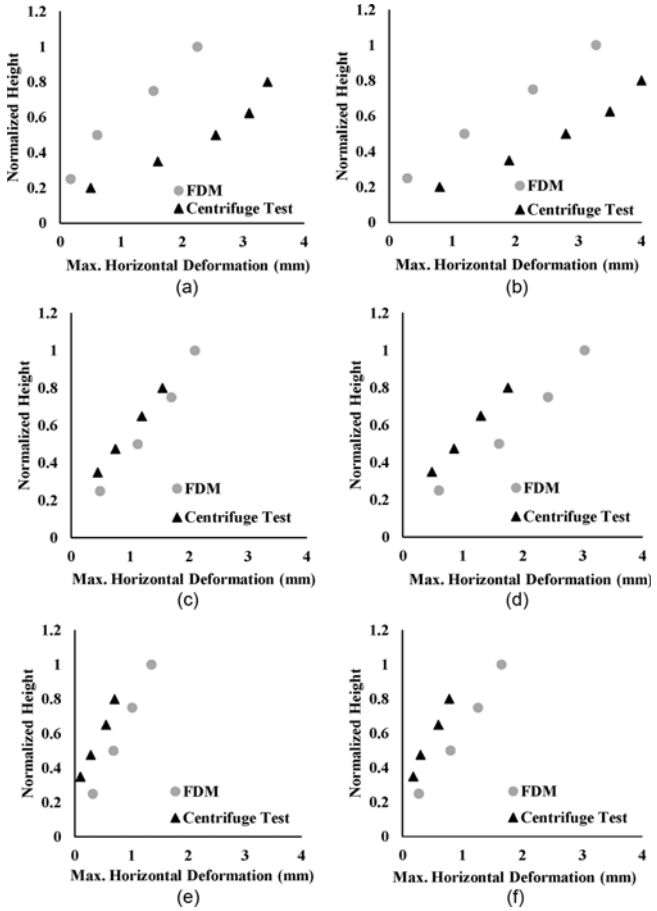

Fig. 5. Maximum Horizontal Deformations of the Side Walls for: (a) PT-1 (E1), (b) PT-1 (E2), (c) PT-2 (E1), (d) PT-2 (E2), (e) PT-3 (E1), (f) PT-3 (E2)

is a three-accelerometer vertical array in a soil column, second shear strain at depth h_i was approximated by second order numerical differentiation suggested by Zeghal and Elgamal (1994):

$$\gamma_{z_i} = \frac{\left[(\delta_{i+1}-\delta_i)\frac{(h_i-h_{i-1})}{(h_{i+1}-h_i)}+(\delta_i-\delta_{i-1})\frac{(h_{i+1}-h_i)}{(h_i-h_{i-1})}\right]}{(h_{i+1}-h_{i-1})} \quad (10)$$

The deformation vectors at the instant of peak negative and positive deformation were shown in Fig. 4. Racking displacements of the model culverts were successfully modeled in the numerical analyses. Maximum racking deformations along the side walls of the culvert for different flexibility ratio and excitation characteristics were presented in Fig. 5. In this figure, vertical axis shows normalized height which is defined as the vertical distance between the base of the box culvert and the relevant wall elevation for the racking displacement data divided by overall wall height. Numerical modeling results exhibit good agreement with the test data for the intermediate stiffness culvert model (*PT-2*). However, there are discrepancies between the test data and analysis results for the most flexible and most rigid culverts. FDM analyses underestimate racking deformations of the most flexible model (*PT-1*), On the other hand, racking deformations

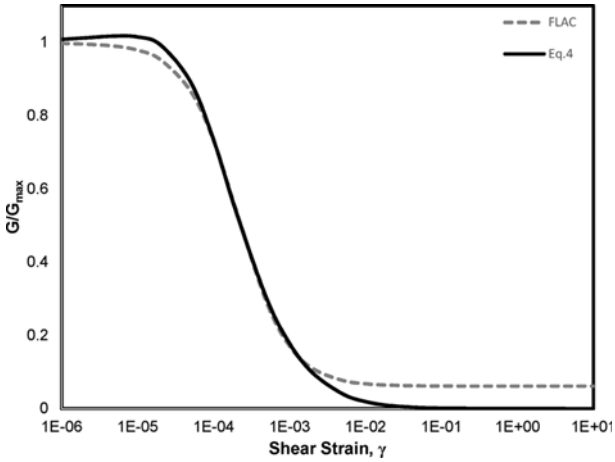

Fig. 6. Comparison of the Actual and Implemented Shear Modulus Degradation Curves

are overestimated for the most rigid model (*PT-3*). The discrepancies between the test data and FDM results may reach up to 50% for the *PT-1*. The discrepancy between the test data and analysis results for the most rigid and most flexible models possibly originates from the numerical representation of the actual shear modulus degradation and the damping behavior of the granular material in the finite difference code. Actual shear modulus degradation and damping curves for the Fontainebleau sand were approximated by sigmoidal functions (Eq. (11)) in FLAC-2D:

$$\frac{G}{G_{max}} = y_0 + \frac{a}{1+exp\left(-\frac{L-x_o}{b}\right)} \quad (11)$$

where $L = log_{10}(\gamma)$ and y_0, x_o, a and b are taken as 0.06154, -3.485, 0.9362 and -0.2993, respectively. As depicted in Fig. 6, sigmoidal fitting curve exhibit higher discrepancies at low and high shear strains while good agreement is observed for the intermediate strain range. As another point, utilization of a single G/G_{max} and D curve representing the behavior of soil for an average confining stress of 28 kPa in the numerical analyses would be one of the causes of the observed discrepancies since the confining stress dependency of the granular materials for the shallow depths considered in the current study may have a more pronounced effect on the dynamic behavior of the soil.

Numerical modeling results indicate that the soil in the vicinity of the *PT-1* (*IFR* = 14.06) are subjected to higher shear strains compared to those of *PT-2* and *PT-3* due to the flexural deformation of the side walls. On the other hand, soils surrounding the *PT-3* (*IFR* = 0.54) exhibit lower shear strains since the flexural deformations are significantly smaller compared to those of *PT-1* and *PT-2*. The discrepancy between the analyses results and the test data for the *PT-1* and *PT-3* model can be explained considering the dynamic shear strain levels of the soils for two models with different flexibilities and the deviation of the fitting curves from the actual shear strain degradation behavior at the

high and low limits of the strain range.

According to Wang (1993), Racking Ratio (RR) of a culvert is defined as:

$$RR = \frac{\Delta_s}{\Delta_{ff}} \tag{12}$$

where Δ_s and Δ_{ff} are the racking deformations of the underground structure and the free field deformation of the ground at the relevant depth as depicted in Fig. 7(a). To calculate the free field deformations of the soil, dynamic free field tests were conducted to determine the acceleration response, displacements and shear strain of free field model ground (Ozkan *et al*., 2013). Similarly, in the numerical modeling part of the current study, free field soil geometries without box culvert were analyzed to estimate the free field shear strains in the soil. The centrifuge test data for free field response and the numerical analyses results were used to determine the racking ratio of the box culverts.

Penzien (2000) suggested the following relationship to estimate the racking ratio of the structure:

$$RR = \frac{4(1-\nu_s)}{1+\alpha_s} \tag{13}$$

$$\alpha_s = (3-4\nu_s)\frac{k_l}{k_{si}} \tag{14}$$

where ν_s is the Poisson's ratio of the soil, k_{si} and k_l are soil and lining stiffness coefficients, respectively. According to Penzien (2000), k_{si} is defined as:

$$k_{si} = \frac{G_S}{H} \tag{15}$$

where G_s is the shear modulus of the surrounding soil at the relevant shear strain and H is the height of the soil medium. The shear modulus values at relevant strains were calculated according to Eqs. (4) to (6). Lining stiffness (k_l) values for three different prototypes tested in this study (Table 3) were calculated through plane strain static analysis of the lining subjected to shear loading as shown in Fig. 7(b).

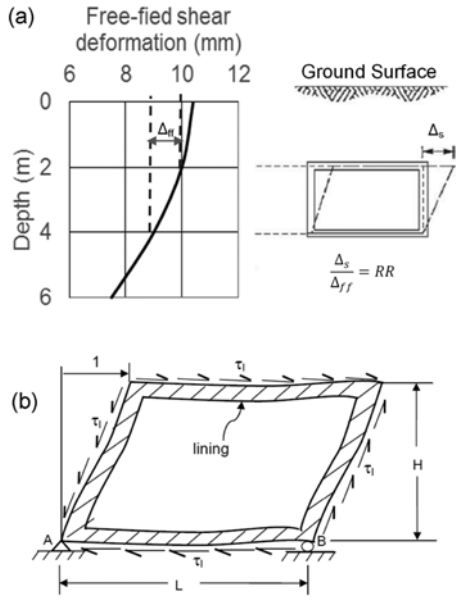

Fig. 7. (a) Racking Ratio of the Box Culvert (Owen and Scholl, 1981), (b) Stiffness Coefficient $k_l = t_l$ for a Rectangular Lining (Penzien, 2000)

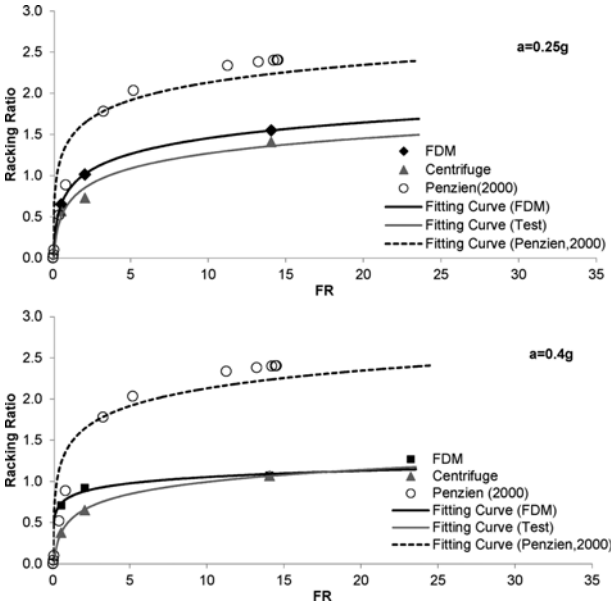

Fig. 8. Variation of Racking Ratio with Respect to Flexibility Ratio

In Fig. 8, racking ratios obtained from numerical analyses were compared with centrifuge test data. Values predicted with the numerical model are in agreement with centrifuge test data. However, it was observed that empirical Penzien's solution is over-estimating the racking deformations of the prototype structure. Penzien (2000) assumes that the wavelength of the shear wave is higher than the height of the tunnel and inertia effects due to soil structure interaction are negligible. On this basis, racking deformation of rectangular underground structure was evaluated under constant shear stress and quasi-static conditions. There are four possible explanations for the over-estimation of the racking ratios with Penzien (2000) Approach:

1. In Fig. 9, lateral soil deformations in the vicinity of the culvert structure at t = 4.42s of the dynamic numerical analysis for the PT-1 culvert model subjected to base excitation of 0.4 g at 3.5 Hz were depicted. In this figure, stress contour legend is given in N/m^2. As can be observed from the figure, arching effect induced in the retained soil by the lateral deformation of the culvert walls has a positive effect, by absorbing a portion of the total unbalanced dynamic force exerted by the backfill and thus causing a reduction in the lateral wall thrust. The positive effect of lateral soil arching on the dynamic earth force was not taken into account in Penzien (2000). It is obvious that flexural deformations of the culvert walls increase as the rigidity of the structure decreases. The highest wall deformations occur at the mid-height of the culvert walls according to numerical analyses

Fig. 9. Lateral Dynamic Earth Pressure Contours Leading to Highest Wall Force for Model PT-1 at 0.4 g and 3.5 Hz Excitation

and centrifuge tests. This translates into a reduction in the lateral soil pressures owing to the lateral soil arching effect induced by the displacements concentrated at the mid-height of the culvert walls.

2. Inertia of the structure is neglected in Penzien Approach however, Huo *et al.* (2005) indicated that shear modulus exhibits little degradation if the structure is more rigid than the ground. This behavior may translate into smaller racking deformations of the structure.
3. Normal stresses acting on the underground structure is neglected. However, frictional forces induced in the top and bottom slabs may have a positive effect on the seismic racking ratios if the structure is not moving in phase with the surrounding soil.
4. In Penzien approach, racking ratio of the structure is evaluated under constant shear stress however, numerical analyses results indicate that shear stress profile significantly changes in relation to the relative movement of the structure with respect to the surrounding soil.

Dynamic lateral forces normalized with at-rest lateral force acting on the side walls were presented in Fig. 10(a) for different IFR values. Within this study, dynamic lateral force is expressed as the total earth thrust acting on the entire area of the side walls during the dynamic excitation phase. Static component of the earth thrust at-rest condition is not deduced from the dynamic lateral force since the pre-excitation static force on the walls of the structure changes depending on the flexibility of the structure and exhibits a non-linear distribution along the wall height.

Numerical analysis results (Fig. 10(a)) indicate that dynamic force may reach up to approximately 2.8 times the theoretical at-rest earth force ($0.5\gamma H^2\{1-\sin\Phi^\circ\}$) for the stiff model (PT-3), whereas for the flexible prototype, this value is only 1.6 times the static earth load. As the flexibility ratio increases, dynamic force decreases owing to the higher flexural deformations of the culvert walls. However, it should be noted that flexibility ratio of the culvert structure is dependent on the soil shear modulus, which is a strain dependent parameter. Thus, $P_{dyn}/P_{at\text{-}rest}$ ratio varies as shear strains within the soil change during dynamic excitation. In Fig. 11, effect of shear strain on the $P_{dyn}/P_{at\text{-}rest}$ ratio was depicted for different prototypes and acceleration amplitudes.

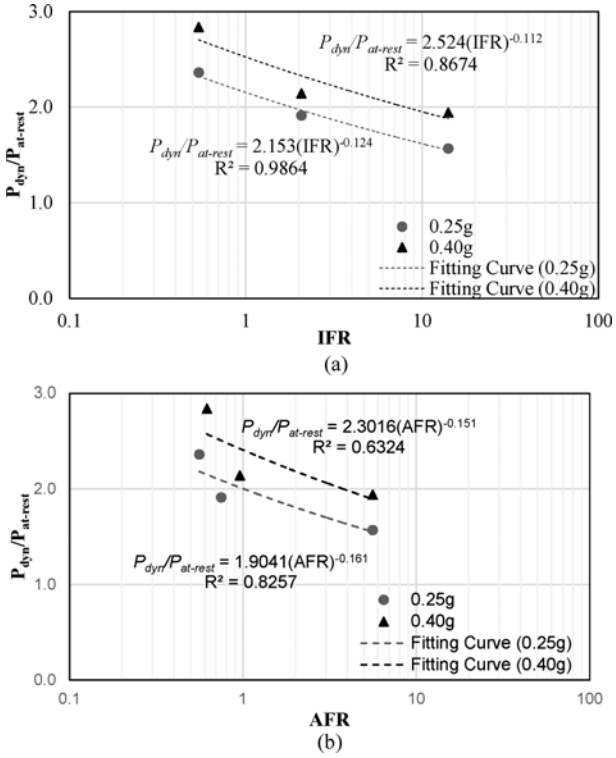

Fig. 10. Maximum Dynamic Earth Pressure Ratio Versus: (a) Initial Flexibility Ratio, (b) Actual Flexibility Ratio

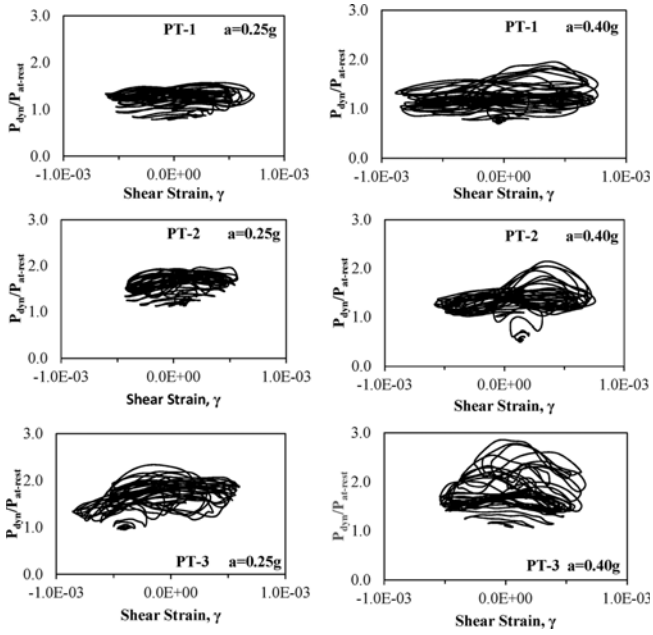

Fig. 11. Variation of Dynamic Earth Pressure Ratio During Dynamic Excitation Phase

The degraded shear modulus values were calculated using Eqs. (4) to (6). It was observed that $P_{dyn}/P_{at\text{-}rest}$ ratio was significantly affected by the momentary relative flexibility of the box culvert. For the most flexible model (PT-1), $P_{dyn}/P_{at\text{-}rest}$ values vary between 0.80 and 1.60 whereas this ratio is observed to be between 0.98 and 2.80 for the most rigid structure (PT-3).

Maximum $P_{dyn}/P_{at\text{-}rest}$ values were replotted against actual flexibility ratios (calculated with degraded shear modulus of the soil this time) in Fig. 10(b). Similar to the behavior observed in Fig. 10(a), a decreasing trend is observed for $P_{dyn}/P_{at\text{-}rest}$ ratio as the actual flexibility ratio decreases.

5. Conclusions

Within the confines of this manuscript, results of a numerical modeling study on the seismic response of shallow-buried box culverts in cohesionless dry soils were presented. Results of the numerical analyses were validated with data obtained from centrifuge modeling study of Ozkan *et al*. (2013). Dimensions of the numerical model used in the finite difference analyses represent prototype dimensions of the small-scale box culvert model subjected to harmonic excitations under 40-g centrifugal acceleration. Dynamic properties of the soils (shear modulus and damping ratio at different strain levels, maximum shear modulus) and structural attributes were similar with those reported by Ozkan *at al.* (2013). Culverts having different wall thicknesses were modeled to investigate the effect of relative flexibility on the dynamic response. Results of the analyses indicate that numerical model may replicate the plane strain dynamic behavior of the actual box culvert prototypes installed at shallow depths in dry cohesionless soils. Racking curves for culverts having different flexibilities were estimated based on numerical modeling results. Good agreement exists between the test data and those predicted with the finite difference method. For the range of excitation characteristics, dynamic force on the sidewalls of the box culvert may reach up to 2.8 times the at-rest lateral stress for the stiff prototype. As flexibility ratio increase, dynamic force decreases as expected. Based on the outputs of the validated numerical analyses, it was observed that dynamic earth pressures on rigid embedded structures may vary significantly during the dynamic excitation due to the degradation in shear modulus of the soils with increasing shear strains. Hence, designing the rigid structure considering the initial flexibility ratio may not be realistic.

As another note, Penzien Approach is too conservative in estimating the racking ratio of the embedded box structure. Depending on the maximum acceleration level, the racking ratios calculated with Penzien Approach may be reduced between 30% and 45%. Based on the results of centrifuge tests and numerical analyses, a significant increase does not occur in the racking ratio for structures having flexibility ratio greater than 10. This effect is more pronounced for higher acceleration amplitudes.

In this study, shear strain levels at the mid-depth of structure varies between 0.001% and 0.2% during dynamic excitations. Hence, racking curves and dynamic pressure ratio values presented within this paper may not be applicable for shear strain levels greater than 0.2%. As a future research, author intends to perform parametric analyses by using the validated numerical model to investigate the effect of yielding characteristics of different soils and the effect of soil liquefaction on the dynamic response of the embedded box structures.

References

AASHTO (2002). *Standard specifications for highway bridges*, American Association of State Highway and Transportation Officials, Seventeenth Edition, Washington, DC, USA.

Bathurst, R. J. and Hatami, K. (1998). "Seismic response analyses of a geosynthetic reinforced soil retaining wall." *Geosynthetics International*, Vol. 5, No. 1, pp. 127-166, DOI: 10.1680/gein.5.0117.

Bobet, A., Fernández, G., and Huo, H. (2008). "A practical iterative procedure to estimate seismic induced deformations of shallow rectangular structures." *Canadian Geotechnical Journal,* Vol. 45, No. 7, pp. 923-938, DOI: 10.1139/T08-026.

Bozorgzadeh, A., Ashford, S. A., and Restrepo, J. I. (2008). "Effect of backfill soil type on stiffness and ultimate capacity of bridge abutments." *Proc., Geotechnical Earthquake Engineering and Soil Dynamics IV Conf*., pp. 1-10.

Debiasi, E., Gajo, A., and Zonta, D. (2013). "On the seismic response of shallow-buried rectangular structures." *Tunnelling and Underground Space Technology*, Vol. 38, pp. 99-113, DOI: 10.1016/j.tust.2013.04.011.

Hardin, B. O. and Drnevich, V. P. (1972). "Shear modulus and damping in soils: Design equations and curves." *J. of Soil Mechanics and Foundation Engineering*, ASCE, Vol. 98, No. SM7, pp. 667-692.

Huo, H., Bobet, A., and Fernandez, G. (2006). "Analytical solution for deep rectangular under-ground structures subjected to far field shear stresses." *Tunnelling and Underground Space Technology*, Vol. 21, No. 6, pp. 613-625, DOI: 10.1016/j.tust.2005.12.135.

Iai, S. (1989). "Similitude for shaking table tests on soil-structure-fluid model in 1 g gravitational field." *Soils and Foundations*, Vol. 29, No. 1, pp. 105-118.

Ishibashi, I. and Zhang, X. (1993). "Unified dynamic shear moduli and damping ratios of sand and clay." *Soils and Foundations*, Vol. 33, No. 1, pp. 182-91, DOI: 10.3208/sandf1972.33.182.

Itasca Consulting Group, Inc. (2008). *FLAC 2D fast lagrangian analysis of the continua version 6.0 dynamic analysis user manual*, Minneapolis, Minnesota.

Matsuo, O., Tsutsumi, T., Yokoyama, K., and Saito, Y. (1998). "Shaking Table Tests and Analysis of Geosynthetic-reinforced Soil Retaining Walls." *Geosynthetics International*, Vol. 5, No. 1, pp. 97-126.

Ozkan, M. Y., Ulgen, D., Saglam, S., Vrettos C., and Chazelas J. L. (2013). *Centrifuge modeling of dynamic behavior of box shaped underground structures in sand: Final report*, Seismic Engineering Research Infrastructures for European Synergies (SERIES), Project No: 227887.

Owen, G. N. and Scholl, R. E. (1981). *Earthquake engineering of large underground structures*, Federal Highway Administration, Report No: FHWA/RD-80/195.

Penzien, J. (2000). "Seismically induced racking of tunnel linings." *Journal of Earthquake Engineering and Structural Dynamics*, Vol. 29, No. 5, pp. 683-691, DOI: 10.1002/(SICI)1096-9845(200005)29:5<683::AID-EQE932> 3.3.CO;2-T.

Plaxis (1998). Plaxis 2D Ver.7 *finite element code for soil and rock analyses,* User's Manual.

Tiwari, B., Ajmera, B., and Kaya, G. (2010). "Shear strength reduction at soil structure interface." *Proc. GeoFlorida 2010 Advances in Analysis, Modeling and Design*, pp. 1747-1756, DOI: 10.1061/41095(365)177.

Ulgen, D. (2011). *An experimental study on the behavior of box-shaped*

culverts buried in sand under dynamic excitations, Ph.D. Dissertation, Middle East Technical University, Ankara, Turkey.

Wald, D. J., Quitoriano, V., Heaton, T. H., and Kanamori, H. (1999). "Relationship between peak ground acceleration, peak ground velocity, and modified mercalli intensity in California." *Earthquake Spectra*, Vol. 15, No. 3, pp. 557-564.

Wang, J. N. (1993). *Seismic design of tunnels*, Parsons Brinckerhof, Inc., Monograph 7.